Journal of Computational Applied Mechanics 2024, 55(3): 440-450

DOI: 10.22059/jcamech.2024.377439.1116

RESEARCH PAPER

Free Vibration of a Tapered Beam by the Aboodh Transform-based Variational Iteration Method

Naveed Anjum [a], Ayesha Rasheed [a], Ji-Huan He [b,c*] , Abdulrahman Ali Alsolami [d]

[a] *Department of Mathematics, Government College University, Faisalabad, Pakistan*
[b] *School of Jia Yang, Zhejiang Shuren University, Hangzhou, Zhejiang, China*
[c] *National Engineering Laboratory for Modern Silk, College of Textile and Engineering, Soochow University, Suzhou, China*
[d] *Department of Mathematics, Faculty of Science, King Abdulaziz University, Jeddah, Saudi Arabia*

Abstract

Physical systems frequently exhibit nonlinear behavior that remains unresolved in the majority of cases. In this study, we employ the Aboodh transform-based variational iteration method (ATVIM) to resolve the nonlinear model of a tapered beam. In order to solve the governing equation, the periodic motion is sought, and the explicit relationship between frequency and amplitude is revealed. The outcomes of the ATVIM approach are compared with those of other prevalent techniques, and a satisfactory concordance is observed between them. This study also provides an analytical approximation of the tapered beam for a detailed understanding of the effects of factors on the nonlinear frequency, which can be beneficial to researchers and engineers working on the analysis and design of structural projects.

Keywords: Aboodh transform, Tapered beam, variational iteration method, amplitude-frequency relationship, nonlinear oscillator.

1. Introduction

The study of nonlinear phenomena is of significant importance, given their prevalence in a multitude of natural systems and engineering applications. These include chaos theory, robotics, material sciences, and biological systems, as evidenced by the extensive literature on the subject [1-5]. An understanding of these phenomena can facilitate the explanation and prediction of complex physical processes, which in turn can lead to the development of new technologies and novel applications. For instance, the advancement of nonlinear optics has resulted in the development of sophisticated laser systems, while nonlinear control theory has facilitated the design of more efficient and robust control systems. One of the most significant developments in structural engineering is the tapered beam.

A tapered beam is a structural element that exhibits a variable cross-sectional profile along its length. The beam may either expand or contract in width and/or depth, resulting in a gradually changing cross-section. It is necessary to examine the nonlinear oscillatory dynamic behaviour of these elements at large amplitudes, as they are commonly used in load-bearing applications such as bridge construction, aeronautical engineering, automobile manufacturing, and other load-bearing applications [6].

The differential equations are the principal instrument utilized to model the nonlinearities inherent in the tapered beam model. Consequently, the nonlinear oscillatory differential equations have received considerable attention. To

* Corresponding author. Tel.: +86-139-1315-2427.
E-mail address: hejihuan@suda.edu.cn

address these vibratory issues, a multitude of analytical and numerical techniques have been proposed. Analytical techniques are more appealing in the context of oscillatory problems because they provide nonlinear frequency and approximate solutions in terms of parameters. There are numerous analytical approaches for nonlinear oscillators, including the variational theory [7-11], the frequency formulation [12-19], the max-min approach [20], the variational iteration method [21], the homotopy perturbation method [22-24].

A nonlinear partial differential equation that exists in both space and time regulates the nonlinear vibration of beams. Consider the tapered beam depicted in Figure 1, the dimensionless governing differential equation is [25]

$$\frac{d^2u}{dt^2}+\left(1+\alpha u^2\right)^{-1}\left[1+\alpha\left(\frac{du}{dt}\right)^2+\beta u^2\right]u=0, \tag{1}$$

where u is displacement, α,β are arbitrary constants and t is time.

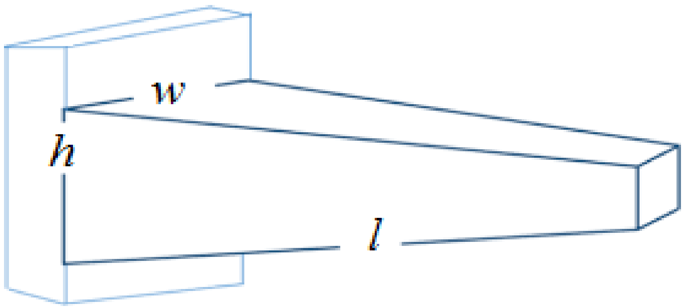

Fig 1: Tapered Beam

This paper introduces a novel approximate analytic technique, the Aboodh transform-based variational iteration method (ATVIM), which represents a significant advancement in the field of variational iteration method.

2. Aboodh transform-based variational iteration method

The VIM was initially developed in the late 1990s [21]. Since its inception, this technique has been employed by numerous individuals to address a range of problems, including initial values, boundary values, linear, and nonlinear problems. In order to employ this technique, a correction functional must be constructed, and the solution must be acquired through an unending sequence that results in a precise response. The application of this strategy to real-world applications may be challenging due to the method's reliance on the knowledge of variational theory [8, 9, 11, 14], which requires an understanding of the Lagrange multiplier.

In 2019, the Laplace transform was incorporated with the variational iteration method, making the identification of the Lagrange multiplier much easier [26]. In this paper, the Aboodh transform [27-29] is used for the same purpose. Let us assume that *f*(*t*) is an exponential continuous piecewise function. In this case, the Aboodh transform is defined as

$$A\left[f(t)\right]=f(v)=\frac{1}{v}\int_0^\infty f(t)e^{-vt}dt,\quad t\ge 0, a_1\le v\le a_2, \tag{2}$$

where $a_1,a_2>0$ can either be infinite or finite. Ref. [31] displays the Aboodh and inverse Aboodh transform of certain functions that are pertinent to this study. The first and second order time derivative of *f*(*t*) by using Aboodh's transform is:

$$A\left[f'(t)\right]=vf(v)-\frac{f(0)}{v}, \tag{3}$$

$$A\left[f''(t)\right]=v^2f(v)-\frac{f'(0)}{v}-f(0), \tag{4}$$

If *T* is any positive integer and *f*(*t*) & *g*(*t*) are piecewise continuous functions over the interval [0,T), then the convolution of *f* and *g* may be represented as

$$(f*g)(t)=\int_0^t f(u)g(t-u)du, \tag{5}$$

The Aboodh transform of the convolution can be represented as:

$$A\left[\left(f*g\right)\left(t\right)\right]=A\left[f\left(t\right)\right]A\left[g\left(t\right)\right]=v\bar{f}\left(v\right)\bar{g}\left(v\right), \tag{6}$$

Now, consider the general nonlinear oscillatory equation:

$$u''+f\left(u\right)=0, \tag{7}$$

We re-write Eq. (7) in the form

$$u''+\omega^2 u+\tilde{g}\left(u\right)=0, \tag{8}$$

where $\tilde{g}\left(u\right)=f\left(u\right)-\omega^2\left(u\right), \omega$ is the frequency and $u(t)$ is a function of time. The variational iteration method's correction functional is expressed as:

$$u_{n+1}\left(t\right)=u_n\left(t\right)+\int_0^t\lambda\left(t-\xi\right)\left\{u_n''\left(\xi\right)+\omega^2 u_n\left(\xi\right)+\tilde{g}\left(u_n\right)\right\}d\xi,\quad n=0,1,2,\cdots\cdots, \tag{9}$$

where λ is general Lagrange multiplier. Now, applying Aboodh transform in Eq. (9), we have

$$\begin{gathered}A\left[u_{n+1}\left(t\right)\right]=A\left[u_n\left(t\right)\right]+A\left[\int_0^t\lambda\left(t-\xi\right)\left\{u_n''\left(\xi\right)+\omega^2 u_n\left(\xi\right)+\tilde{g}\left(u_n\right)\right\}d\xi\right],\\ A\left[u_{n+1}\left(t\right)\right]=A\left[u_n\left(t\right)\right]+A\left[\lambda\left(t\right)*\left\{u_n''\left(t\right)+\omega^2 u_n\left(t\right)+\tilde{g}\left(u_n\right)\right\}\right],\\ A\left[u_{n+1}\left(t\right)\right]=A\left[u_n\left(t\right)\right]+vA\left[\lambda\left(t\right)\right]A\left[u_n''\left(t\right)+\omega^2 u_n\left(t\right)+\tilde{g}\left(u_n\right)\right],\\ A\left[u_{n+1}\left(t\right)\right]=A\left[u_n\left(t\right)\right]+vA\left[\lambda\left(t\right)\right]\left\{\left(v^2+\omega^2\right)A\left[u_n\left(t\right)\right]-\frac{u_n'\left(0\right)}{v}-u_n\left(0\right)+A\left[\tilde{g}\left(u_n\right)\right]\right\}.\end{gathered} \tag{10}$$

Attempting to make Eq. (10) stationary with respect to $u_n\left(t\right)$ allows for the best value of λ to be obtained; this requires

$$\begin{aligned}&\frac{\delta}{\delta u_n}A\left[u_{n+1}\left(t\right)\right]=\frac{\delta}{\delta u_n}A\left[u_n\left(t\right)\right]\\ &+\frac{\delta}{\delta u_n}vA\left[\lambda\left(t\right)\right]\left\{\left(v^2+\omega^2\right)A\left[u_n\left(t\right)\right]-\frac{u_n'\left(0\right)}{v}-u_n\left(0\right)+A\left[\tilde{g}\left(u_n\right)\right]\right\},\\ &=\left\{1+\left(v^2+\omega^2\right)vA\left[\lambda\left(t\right)\right]\right\}\frac{\delta}{\delta u_n}A\left[u_n\left(t\right)\right]\\ &=0.\end{aligned} \tag{11}$$

From above equation we have

$$\begin{aligned}vA\left[\lambda\left(t\right)\right]&=-\frac{1}{\left(v^2+\omega^2\right)},\\ A\left[\lambda\left(t\right)\right]&=-\frac{1}{v\left(v^2+\omega^2\right)}.\end{aligned} \tag{12}$$

We assume in preceding derivation that

$$\frac{\delta A\left[u_n\left(t\right)\right]}{\delta u_n}=0. \tag{13}$$

By employing inverse Aboodh transform on Eq. (12) yields

$$\lambda\left(t\right)=-\frac{1}{\omega}\left[\frac{\omega}{v\left(v^2+\omega^2\right)}\right],$$

$$\lambda(t) = -\frac{1}{\omega}\sin \omega t. \tag{14}$$

As a result, we can find the Lagrange multiplier considerably more quickly than we could using variational theory. The approximate solution is given by using the Lagrange multiplier in Eq. (10) as follows:

$$A\left[u_{n+1}(t)\right] = A\left[u_n(t)\right] - \frac{1}{\omega}A\left[\sin \omega t * \left\{u_n''(t) + \omega^2 u_n(t) + \tilde{g}(u_n)\right\}\right],$$

$$u_{n+1}(t) = A^{-1}\left[A\left[u_n(t)\right] - \frac{v}{\omega}A\left[\sin \omega t\right]A\left[u_n''(t) + \omega^2 u_n(t) + \tilde{g}(u_n)\right]\right]. \tag{15}$$

From Eq. (15), we can obtain a relationship between ω and A by mean of no secular term in u_{n+1}.

3. Approximate solution

Consider the general form of tapered beam [6, 10].

$$u'' + \frac{u + \alpha u^3 + \beta u\left(u'\right)^2}{1 + \beta u^2}, \tag{16}$$

with basic conditions, we have

$$u(0) = A \text{ and } u'(0) = 0.$$

where A stands for the highest amplitude.

Eq. (16) may be represented as follows:

$$\left(1 + \beta u^2\right)u'' + u + \alpha u^3 + \beta u\left(u'\right)^2 = 0. \tag{17}$$

Aboodh transform-based variational iteration method (ATVIM) is used to obtain the correctional form for Eq. (17), which results in the form.

$$u''(t) + \omega^2 u(t) + \tilde{g}(u) = 0, \tag{18}$$

where $\tilde{g}(u) = \left(1 - \omega^2\right)u(t) + \alpha u^3(t) + \beta u(t)\left(u'(t)\right)^2 + \beta u^2(t)u''(t)$.

We have the following iterative formula:

$$u_{n+1}(t) = u_n(t) - \int_0^t \frac{1}{\omega}\left[\sin(t-\xi)\left\{u_n''(\xi) + u_n(\xi) + \alpha u_n^3(\xi)\right\}d\xi\right]$$
$$-\int_0^t \frac{1}{\omega}\left[\sin(t-\xi)\left\{\beta u_n(\xi)\left(u_n'(\xi)\right)^2 + \beta u_n^2(\xi)u_n''(\xi)\right\}d\xi\right],$$

On both sides, using the Aboodh transform, we have

$$\begin{aligned}
A\left[u_{n+1}(t)\right] &= A\left[u_n(t)\right] - \frac{1}{\omega}A\left[\int_0^t \sin(t-\xi)\left\{u_n''(\xi) + u_n(\xi) + \alpha u_n^3(\xi)\right\}d\xi\right] \\
&- \frac{1}{\omega}A\left[\int_0^t \sin(t-\xi)\left\{\beta u_n(\xi)\left(u_n'(\xi)\right)^2 + \beta u_n^2(\xi)u_n''(\xi)\right\}d\xi\right] \\
&= A\left[u_n(t)\right] - \frac{1}{\omega}\left\{A\left[\sin(t-\xi)\right] * A\left[u_n''(\xi) + u_n(\xi) + \alpha u_n^3(\xi)\right]\right\} \\
&- \frac{1}{\omega}\left\{A\left[\sin(t-\xi)\right] * A\left[\beta u_n(\xi)\left(u_n'(\xi)\right)^2 + \beta u_n^2(\xi)u_n''(\xi)\right]\right\} \\
&= A\left[u_n(t)\right] - \frac{v}{\omega}\left\{A\left[\sin(t)\right]A\left[u_n''(t) + u_n(t) + \alpha u_n^3(t)\right]\right\} \\
&- \frac{v}{\omega}\left\{A\left[\sin(t)\right]A\left[\beta u_n(t)\left(u_n'(t)\right)^2 + \beta u_n^2(t)u_n''(t)\right]\right\}
\end{aligned} \tag{19}$$

For $n=0,$ the above equation becomes

$$A\left[u_1(t)\right]=A\left[u_0(t)\right]-\frac{v}{\omega}\left\{A[\sin\omega t]A\left[u_0''(t)+u_0(t)+\alpha u_0^3(t)\right]\right\}$$
$$-\frac{v}{\omega}\left\{A[\sin\omega t]A\left[\beta u_0(t)\left(u_0'(t)\right)^2+\beta u_0^2(t)u_0''(t)\right]\right\}. \tag{20}$$

By using basic conditions, we choose

$$u_0(t)=A\cos\omega t. \tag{21}$$

We have

$$A\left[u_1(t)\right]=A[\cos\omega t]-\frac{v}{\omega}A[\sin\omega t]A\left[\cos\omega t\left(A-A^2\omega^2+\frac{3}{4}A^3\alpha-\frac{1}{2}A^3\beta\omega^2\right)\right]$$
$$-\frac{v}{\omega}A[\sin\omega t]A\left[\cos 3\omega t\left(\frac{1}{4}A^3\alpha-\frac{1}{2}A^3\beta\omega^2\right)\right]$$
$$=A[\cos\omega t]-\frac{v}{\omega}A[\sin\omega t]A[\cos\omega t]\left\{A-A^2\omega^2+\frac{3}{4}A^3\alpha-\frac{1}{2}A^3\beta\omega^2\right\}$$
$$-\frac{v}{\omega}A[\sin\omega t]A[\cos 3\omega t]\left\{\frac{1}{4}A^3\alpha-\frac{1}{2}A^3\beta\omega^2\right\}. \tag{22}$$

Applying Aboodh inverse transform, we have

$$u_1(t)=\cos\omega t-\frac{1}{\omega}\left(\frac{1}{2}t\sin\omega t\right)\left\{A-A^2\omega^2+\frac{3}{4}A^3\alpha-\frac{1}{2}A^3\beta\omega^2\right\}$$
$$-\frac{1}{\omega}\left(\frac{\cos\omega t-\cos 3\omega t}{8\omega}\right)\left\{\frac{1}{4}A^3\alpha-\frac{1}{2}A^3\beta\omega^2\right\}. \tag{23}$$

In Eq. (23) there is no secular term that implies

$$\frac{1}{\omega}\left\{A-A^2\omega^2+\frac{3}{4}A^3\alpha-\frac{1}{2}A^3\beta\omega^2\right\}=0. \tag{24}$$

This leads to the following result:

$$\omega=\sqrt{\frac{4+3\alpha A^2}{4+2\beta A^2}}. \tag{25}$$

Hence, the approximate solution is

$$u_1(t)=\cos\omega t-\frac{1}{\omega}\left(\frac{\cos\omega t-\cos 3\omega t}{8\omega}\right)\left\{\frac{1}{4}A^3\alpha-\frac{1}{2}A^3\beta\omega^2\right\}$$
$$=\left[1-\frac{1}{8\omega^2}\left(\frac{1}{4}A^3\alpha-\frac{1}{2}A^3\beta\omega^2\right)\right]\cos\omega t+\frac{1}{8\omega^2}\left(\frac{1}{4}A^3\alpha-\frac{1}{2}A^3\beta\omega^2\right)\cos 3\omega t. \tag{26}$$

In order to determine the natural frequency and associated displacement of tapered beams, which serve as indicators of the ATVIM's accuracy, the previously described processes are used. The findings from the ATVIM are compared in the table with the precise outcomes for various values of the parameters A,α and $\beta.$ The first-order analytical estimations for $A=0.1,\alpha=0.1,\beta=0.1$ have a relative error of analytical methods of 0.278% as shown in Table 1.

By contrasting the time period oscillatory displacement behavior for tapered beams with exact calculations, as shown in Figs. 2-4, the precision of these approximative analytical methodologies is further demonstrated and confirmed. The system travels regularly, and the magnitude of the vibration depends on the initial conditions, as shown in Figs. 2, 3, and 4.

Table 1: A comparison of frequency related to different system parameters [6]

(A,α,β)	ω_{EX}	ω_{VIM}	ω_{MMA}	ω_{HA}	ε_{VIM}	ε_{MMA}	ε_{HA}
(0.1,0.1,0.1)	0.9973	1.0001	1.0002	1.0001	0.2777%	0.2877%	0.2777%
(0.2,0.1,0.1)	0.9973	1.0005	1.0007	1.0005	0.3178%	0.3379%	0.3178%
(0.3,0.1,0.1)	0.9973	1.0011	1.0015	1.0011	0.3780%	0.4181%	0.3780%
(0.3,0.1,0.2)	0.9973	0.9989	1.0045	1.0045	0.1574%	0.7189%	0.7189%
(0.3,0.2,0.2)	0.9973	1.0022	1.0030	1.0022	0.4883%	0.5685%	0.4883%
(0.3,0.3,0.3)	0.9973	1.0033	1.0044	1.0033	0.5985%	0.7088%	0.5985%
(0.4,0.1,0.1)	0.9973	1.0020	1.0026	1.0020	0.4682%	0.5284%	0.4682%
(0.4,0.2,0.3)	0.9973	1.0000	1.0105	1.0098	0.2677%	1.3205%	1.2503%
(0.4,0.6,0.7)	1.0150	1.0075	1.0205	1.0170	0.7438%	0.5369%	0.1921%
(0.5,0.1,0.1)	0.9973	1.0031	1.0041	1.0031	0.5785%	0.6788%	0.5785%
(0.6,0.1,0.1)	0.9973	1.0044	1.0059	1.0044	0.7088%	0.8592%	0.7088%
(0.9,0.1,0.1)	1.0150	1.0097	1.0131	1.0097	0.5270%	0.1921%	0.5270%
(1,0.09,0.1)	1.0150	1.0083	1.0176	1.0143	0.6649%	0.2512%	0.0738%
(1,0.2,0.3)	0.9973	1	1.0607	1.0553	0.2677%	6.3539%	5.8125%
(1,0.3,0.4)	1.0150	1.0104	1.0731	1.0632	0.4581%	5.7189%	4.7436%
(1,0.4,0.5)	1.0300	1.0198	1.0847	1.0704	0.9931%	5.3076%	3.9193%
(1,0.5,0.6)	1.0300	1.0284	1.0954	1.0770	0.1582%	6.3464%	4.5600%
(2,0.09,0.1)	1.0300	1.0288	1.0635	1.0496	0.1194%	3.2494%	1.8999%
(2,0.1,0.1)	1.0472	1.0408	1.0572	1.0408	0.6111%	0.9549%	0.6111%
(2,0.2,0.3)	1.0150	1	1.1921	1.1650	1.4826%	17.4424%	14.7726%
(2,0.3,0.4)	1.0472	1.0274	1.2150	1.1726	1.8907%	16.0236%	11.9747%
(2,0.5,0.6)	1.1023	1.0660	1.2490	1.1832	3.2939%	13.3075%	7.3382%

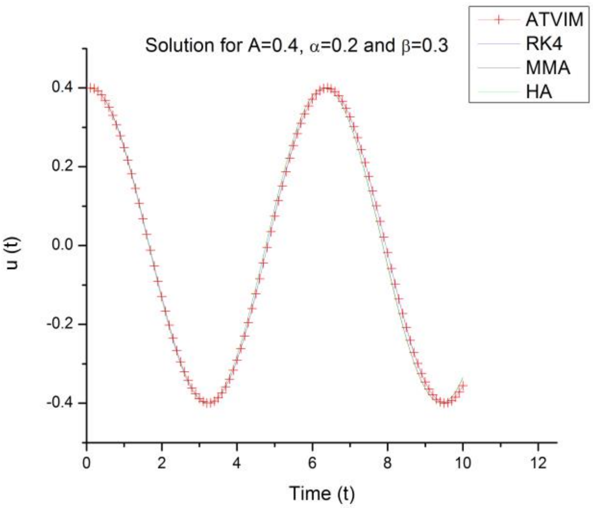

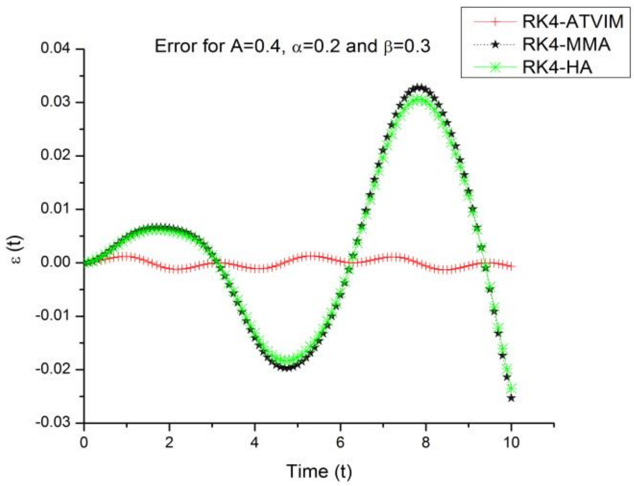

Fig 2: A comparative analysis of the analytical and enhanced solutions for the case when *A*=0.4, *α*=0.2 and *β*=0.3

We exhibit the accurate displacement for the parameter sets A=0.4, α=0.2 and β=0.3 from the numerical solutions for RK4 (solid line), ATVIM (red plus sign), MMA (black solid line), and HA (green solid line) on the left side of Figure 2. It is discovered that, within the range of time and parameter sets taken into consideration for this research, the approximations for the displacement of the tapered beam closely resemble those obtained from the RK4. The accuracy of the results provided by ATVIM, MMA, and HA in this specific case is nearly identical. On the right side of Figure 2, we also show errors against time for the identical value parameters. The ATVIM error (the disparity between the RK4 results and the ATVIM), the MMA error (the difference between the RK4 outcome and the MMA), and the HA error (the distinction between the RK4 conclusion and the HA) are each indicated by a red plus sign with straight lines, a black five-pointed star with dotted lines, and a green six-pointed star with solid lines, respectively. Even while it is certain that flaws are minor, it is given that the ATVIM is weaker than the MMA and HA.

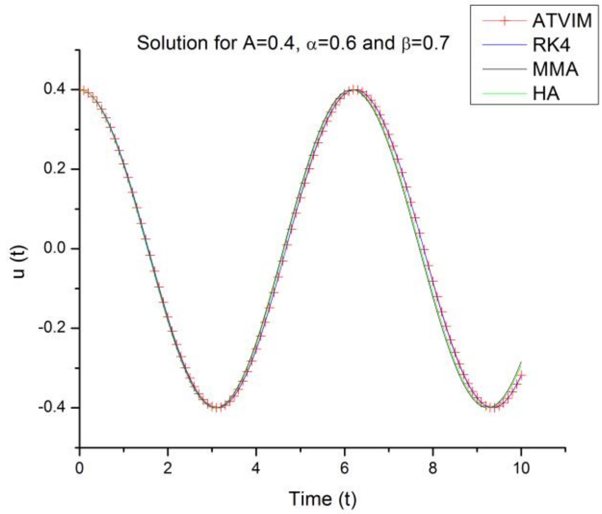

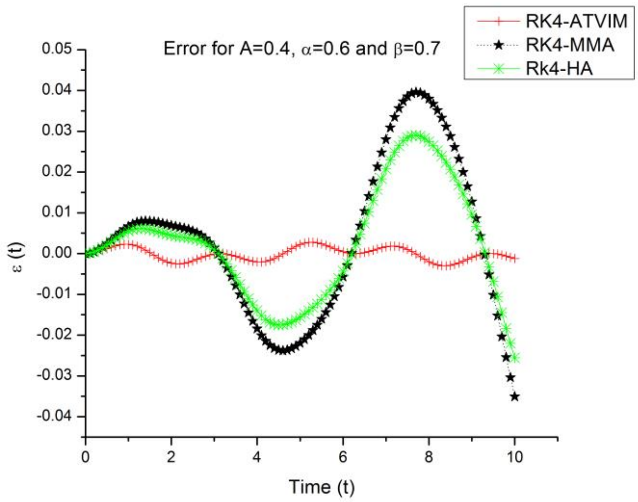

Fig 3: Comparison of the approximate solution for the case when A=0.4, α=0.6 and β=0.7

For the parameter set A=0.4, α=0.6 and β=0.7 on the left side of Figure 3, we plot the precise displacement from the computations RK4 (solid line), ATVIM (plus sign in red), MMA (black solid line), and HA (green solid line). For the range of time and parameter sets taken into consideration for the present study, it is discovered that the estimations for the displacement of the tapered beam closely resemble those obtained from the RK4. The reliability of the outcomes presented by ATVIM, MMA, and HA, in this case, is nearly the same. On the right side of Figure 3, we additionally demonstrate lapses against time for the same value parameters. The ATVIM error (the distinction between the RK4 conclusion and the ATVIM), the MMA error (disparities between the RK4 results and the MMA), and the HA error (a distinction between the RK4 outcome and the HA) are each symbolized by a red plus sign with straight lines, a black five-pointed star with dotted lines, and a green six-pointed star with solid lines, respectively. It is certain, though, that the ATVIM is stronger than the MMA and HA.

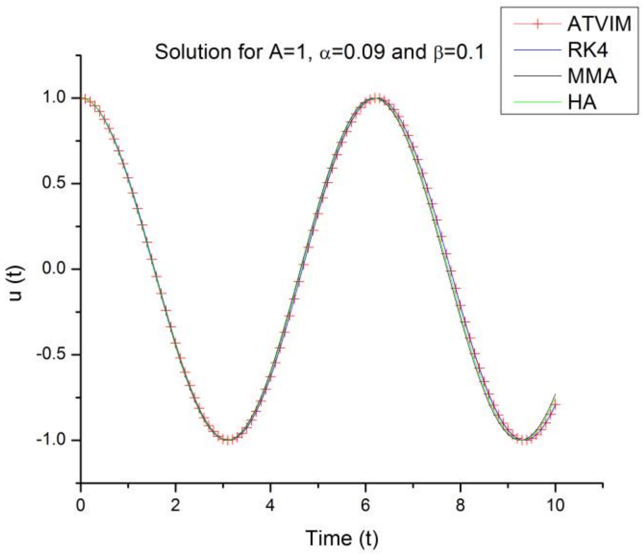

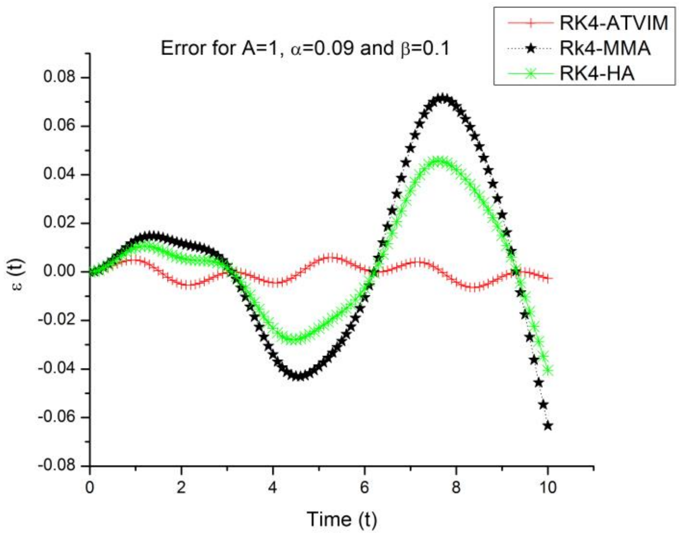

Fig 4: The enhanced solution for the case when A=1, α=0.09 and β=0.1

In Figure 4, we demonstrate the accurate displacement from the computational results RK4 (solid line), ATVIM (plus sign in red), MMA (black solid line), and HA (green solid line) for the parameter set A=1, α=0.09 and β=0.1.

For the range of times and parameter sets taken into consideration for the present research, it turns out that the predictions for the displacement of the tapered beam are very comparable to those obtained from the RK4. The outcomes obtained through ATVIM, MMA, and HA have accuracy levels that are quite similar in this case. For the same value parameters, we also display erroneous against time on Figure 4's right side. The ATVIM error (difference between the RK4 results and the ATVIM), the MMA error (difference between the RK4 conclusion and the MMA), and the HA error (difference between the RK4 outcome and the HA), respectively, are represented by a red plus sign with straight lines, a black five-pointed star with dotted lines, and a green six-pointed star with solid lines. It ensures that the ATVIM is better than MMA and HA.

In figures 5 and 6, for small values α and β, the impact of these parameters on the frequency associated with various amplitude parameters has been investigated.

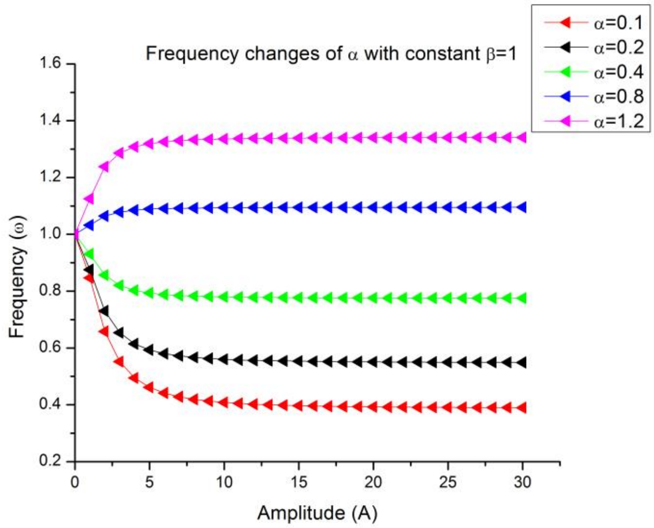

Fig 5: The comparison of the frequency associated with different amplitudes and $\beta = 1$.

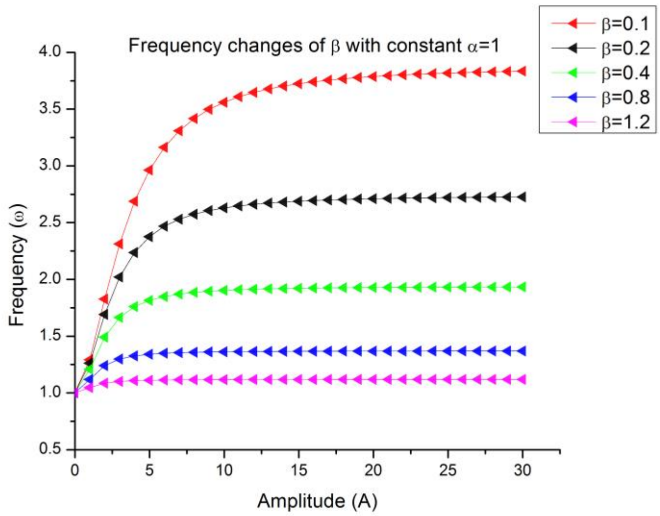

Fig 6: The contrast of frequency for different amplitudes and $\alpha = 1$.

4. Conclusion

The governing equations for the nonlinear oscillations of tapered beams were resolved in the current study using the ATVIM. The analytical results provide a thorough and insightful understanding of the impacts of system elements and beginning circumstances. Analytical outcomes also provide a frame of reference that other computational methods might use to validate and ensure precision. ATVIM can be used to tackle both strong and moderate nonlinear situations. This technology's accuracy over the entire spectrum of oscillation values for amplitude is its best quality. It may also be employed to resolve advanced, conservative nonlinear oscillators. The components of the ATVIM solutions are easily calculable and fast converge. Also, it can be seen that ATVIM produces results that require less computer work than those of other analytical techniques and that only one iteration is enough to reach valid conclusions. The application of the ATVIM in the large amplitude nonlinear oscillation problem taken into consideration in this work serves as an example of the efficiency of those methods in resolving nonlinear oscillation problems.

References

[1] S. A. Faghidian, A. Tounsi, DYNAMIC CHARACTERISTICS OF MIXTURE UNIFIED GRADIENT ELASTIC NANOBEAMS, *Facta Universitatis, Series: Mechanical Engineering*, Vol. 20, pp. 539, 11/30, 2022.

[2] Q. Ain, D. Tian, N. Anjum, Fractal N/MEMS: From pull-in instability to pull-in stability, *Fractals*, Vol. 29, 10/18, 2020.
[3] D. Tian, C.-H. He, A fractal micro-electromechanical system and its pull-in stability, *Journal of Low Frequency Noise, Vibration and Active Control*, Vol. 40, No. 3, pp. 1380-1386, 2021.
[4] C. He, Q. Zhang, S. Tao, C. Zhao, C. Zhao, W. Su, Y. J. Dappe, R. J. Nichols, L. Yang, Carbon-contacted single molecule electrical junctions, *Physical Chemistry Chemical Physics*, Vol. 20, No. 38, pp. 24553-24560, 2018.
[5] C.-H. He, T. S. Amer, D. Tian, A. F. Abolila, A. A. Galal, Controlling the kinematics of a spring-pendulum system using an energy harvesting device, *Journal of Low Frequency Noise, Vibration and Active Control*, Vol. 41, No. 3, pp. 1234-1257, 2022.
[6] M. Bayat, I. Pakar, M. Bayat, Analytical study on the vibration frequencies of tapered beams, *Latin American Journal of Solids and Structures*, Vol. 8, pp. 149-162, 06/01, 2011.
[7] J.-H. He, Variational approach for nonlinear oscillators, *Chaos, Solitons & Fractals*, Vol. 34, No. 5, pp. 1430-1439, 2007/12/01/, 2007.
[8] Y.-T. Zuo, VARIATIONAL PRINCIPLE FOR A FRACTAL LUBRICATION PROBLEM, *Fractals*, 05/23, 2024.
[9] C.-H. He, A variational principle for a fractal nano/microelectromechanical (N/MEMS) system, *International Journal of Numerical Methods for Heat & Fluid Flow*, Vol. 33, No. 1, pp. 351-359, 2022.
[10] K.-L. WANG, C.-H. HE, A REMARK ON WANG'S FRACTAL VARIATIONAL PRINCIPLE, *Fractals*, Vol. 27, No. 08, pp. 1950134, 2019.
[11] C.-H. He, C. Liu, Variational principle for singular waves, *Chaos, Solitons & Fractals*, Vol. 172, pp. 113566, 07/01, 2023.
[12] J.-H. He, The simplest approach to nonlinear oscillators, *Results in Physics*, Vol. 15, pp. 102546, 08/01, 2019.
[13] J.-H. He, The simpler, the better: Analytical methods for nonlinear oscillators and fractional oscillators, *Journal of Low Frequency Noise, Vibration and Active Control*, Vol. 38, No. 3-4, pp. 1252-1260, 2019.
[14] H. Ma, SIMPLIFIED HAMILTONIAN-BASED FREQUENCY-AMPLITUDE FORMULATION FOR NONLINEAR VIBRATION SYSTEMS, *Facta Universitatis, Series: Mechanical Engineering*, Vol. 20, pp. 445, 07/28, 2022.
[15] Y. Tian, Frequency formula for a class of fractal vibration system, *Reports in Mechanical Engineering*, Vol. 3, No. 1, pp. 55-61, 2022.
[16] J.-Y. Niu, G.-Q. Feng, K. A. Gepreel, A simple frequency formulation for fractal–fractional non-linear oscillators: A promising tool and its future challenge, *Frontiers in Physics*, Vol. 11, 2023-March-16, 2023. English
[17] G. Feng, A CIRCULAR SECTOR VIBRATION SYSTEM IN A POROUS MEDIUM, *Facta Universitatis, Series: Mechanical Engineering*, 2023.
[18] Y. El-dib, A review of the frequency-amplitude formula for nonlinear oscillators and its advancements, *Journal of Low Frequency Noise Vibration and Active Control*, pp. 1-33, 04/05, 2024.
[19] C.-H. HE, C. LIU, A MODIFIED FREQUENCY–AMPLITUDE FORMULATION FOR FRACTAL VIBRATION SYSTEMS, *Fractals*, Vol. 30, No. 03, pp. 2250046, 2022.
[20] J.-H. He, Max-min approach to nonlinear oscillators, *International Journal of Nonlinear Sciences and Numerical Simulation*, Vol. 9, No. 2, pp. 207-210, 2008.
[21] J.-H. He, Variational iteration method–a kind of non-linear analytical technique: some examples, *International journal of non-linear mechanics*, Vol. 34, No. 4, pp. 699-708, 1999.
[22] J.-H. He, Homotopy perturbation technique, *Computer methods in applied mechanics and engineering*, Vol. 178, No. 3-4, pp. 257-262, 1999.
[23] J.-H. He, Y. O. El-Dib, The reducing rank method to solve third-order Duffing equation with the homotopy perturbation, *Numerical Methods for Partial Differential Equations*, Vol. 37, No. 2, pp. 1800-1808, 2021.
[24] Y. El-dib, A heuristic review on the homotopy perturbation method for non-conservative oscillators, 05/07, 2022.
[25] D. Goorman, Free vibrations of beams and shafts, *Appl. Mech., ASME*, Vol. 18, pp. 135-139, 1975.
[26] N. Anjum, J.-H. He, Laplace transform: Making the variational iteration method easier, *Applied Mathematics Letters*, Vol. 92, pp. 134-138, 2019/06/01/, 2019.
[27] K. Manimegalai, S. Zephania CF, P. Bera, P. Bera, S. Das, T. Sil, Study of strongly nonlinear oscillators using the Aboodh transform and the homotopy perturbation method, *The European Physical Journal Plus*, Vol. 134, pp. 1-10, 2019.

[28] N. Al-Rashidi, Innovative approaches to fractional modeling: Aboodh transform for the Keller-Segel equation, *AIMS Mathematics*, Vol. 9, No. 6, pp. 14949-14981, 2024.

[29] H. Ji-Huan, N. Anjum, H. Chun-Hui, A. A. Alsolami, BEYOND LAPLACE AND FOURIER TRANSFORMS Challenges and Future Prospects, *Thermal Science*, Vol. 27, 2023.